Ratios of Multijet Cross Sections in $p\bar{p}$ Collisions at $\sqrt{s} = 1.8$ TeV

B. Abbott,[50] M. Abolins,[47] V. Abramov,[23] B. S. Acharya,[15] D. L. Adams,[57] M. Adams,[34] G. A. Alves,[2] N. Amos,[46] E. W. Anderson,[39] M. M. Baarmand,[52] V. V. Babintsev,[23] L. Babukhadia,[52] A. Baden,[43] B. Baldin,[33] P. W. Balm,[18] S. Banerjee,[15] J. Bantly,[56] E. Barberis,[26] P. Baringer,[40] J. F. Bartlett,[33] U. Bassler,[11] A. Bean,[40] M. Begel,[51] A. Belyaev,[22] S. B. Beri,[13] G. Bernardi,[11] I. Bertram,[24] A. Besson,[9] V. A. Bezzubov,[23] P. C. Bhat,[33] V. Bhatnagar,[13] M. Bhattacharjee,[52] G. Blazey,[35] S. Blessing,[31] A. Boehnlein,[33] N. I. Bojko,[23] F. Borcherding,[33] A. Brandt,[57] R. Breedon,[27] G. Briskin,[56] R. Brock,[47] G. Brooijmans,[33] A. Bross,[33] D. Buchholz,[36] M. Buehler,[34] V. Buescher,[51] V. S. Burtovoi,[23] J. M. Butler,[44] F. Canelli,[51] W. Carvalho,[3] D. Casey,[47] Z. Casilum,[52] H. Castilla-Valdez,[17] D. Chakraborty,[52] K. M. Chan,[51] S. V. Chekulaev,[23] D. K. Cho,[51] S. Choi,[30] S. Chopra,[53] J. H. Christenson,[33] M. Chung,[34] D. Claes,[48] A. R. Clark,[26] J. Cochran,[30] L. Coney,[38] B. Connolly,[31] W. E. Cooper,[33] D. Coppage,[40] M. A. C. Cummings,[35] D. Cutts,[56] O. I. Dahl,[26] G. A. Davis,[51] K. Davis,[25] K. De,[57] K. Del Signore,[46] M. Demarteau,[33] R. Demina,[41] P. Demine,[9] D. Denisov,[33] S. P. Denisov,[23] S. Desai,[52] H. T. Diehl,[33] M. Diesburg,[33] G. Di Loreto,[47] S. Doulas,[45] P. Draper,[57] Y. Ducros,[12] L. V. Dudko,[22] S. Duensing,[19] S. R. Dugad,[15] A. Dyshkant,[23] D. Edmunds,[47] J. Ellison,[30] V. D. Elvira,[33] R. Engelmann,[52] S. Eno,[43] G. Eppley,[59] P. Ermolov,[22] O. V. Eroshin,[23] J. Estrada,[51] H. Evans,[49] V. N. Evdokimov,[23] T. Fahland,[29] S. Feher,[33] D. Fein,[25] T. Ferbel,[51] H. E. Fisk,[33] Y. Fisyak,[53] E. Flattum,[33] F. Fleuret,[26] M. Fortner,[35] K. C. Frame,[47] S. Fuess,[33] E. Gallas,[33] A. N. Galyaev,[23] P. Gartung,[30] V. Gavrilov,[21] R. J. Genik II,[24] K. Genser,[33] C. E. Gerber,[34] Y. Gershtein,[56] B. Gibbard,[53] R. Gilmartin,[31] G. Ginther,[51] B. Gómez,[5] G. Gómez,[43] P. I. Goncharov,[23] J. L. González Solís,[17] H. Gordon,[53] L. T. Goss,[58] K. Gounder,[30] A. Goussiou,[52] N. Graf,[53] G. Graham,[43] P. D. Grannis,[52] J. A. Green,[39] H. Greenlee,[33] S. Grinstein,[1] L. Groer,[49] P. Grudberg,[26] S. Grünendahl,[33] A. Gupta,[15] S. N. Gurzhiev,[23] G. Gutierrez,[33] P. Gutierrez,[55] N. J. Hadley,[43] H. Haggerty,[33] S. Hagopian,[31] V. Hagopian,[31] K. S. Hahn,[51] R. E. Hall,[28] P. Hanlet,[45] S. Hansen,[33] J. M. Hauptman,[39] C. Hays,[49] C. Hebert,[40] D. Hedin,[35] A. P. Heinson,[30] U. Heintz,[44] T. Heuring,[31] R. Hirosky,[34] J. D. Hobbs,[52] B. Hoeneisen,[8] J. S. Hoftun,[56] S. Hou,[46] Y. Huang,[46] A. S. Ito,[33] S. A. Jerger,[47] R. Jesik,[37] K. Johns,[25] M. Johnson,[33] A. Jonckheere,[33] M. Jones,[32] H. Jöstlein,[33] A. Juste,[33] S. Kahn,[53] E. Kajfasz,[10] D. Karmanov,[22] D. Karmgard,[38] R. Kehoe,[38] S. K. Kim,[16] B. Klima,[33] C. Klopfenstein,[27] B. Knuteson,[26] W. Ko,[27] J. M. Kohli,[13] A. V. Kostritskiy,[23] J. Kotcher,[53] A. V. Kotwal,[49] A. V. Kozelov,[23] E. A. Kozlovsky,[23] J. Krane,[39] M. R. Krishnaswamy,[15] S. Krzywdzinski,[33] M. Kubantsev,[41] S. Kuleshov,[21] Y. Kulik,[52] S. Kunori,[43] V. E. Kuznetsov,[30] G. Landsberg,[56] A. Leflat,[22] F. Lehner,[33] J. Li,[57] Q. Z. Li,[33] J. G. R. Lima,[3] D. Lincoln,[33] S. L. Linn,[31] J. Linnemann,[47] R. Lipton,[33] A. Lucotte,[52] L. Lueking,[33] C. Lundstedt,[48] A. K. A. Maciel,[35] R. J. Madaras,[26] V. Manankov,[22] H. S. Mao,[4] T. Marshall,[37] M. I. Martin,[33] R. D. Martin,[34] K. M. Mauritz,[39] B. May,[36] A. A. Mayorov,[37] R. McCarthy,[52] J. McDonald,[31] T. McMahon,[54] H. L. Melanson,[33] X. C. Meng,[4] M. Merkin,[22] K. W. Merritt,[33] C. Miao,[56] H. Miettinen,[59] D. Mihalcea,[55] A. Mincer,[50] C. S. Mishra,[33] N. Mokhov,[33] N. K. Mondal,[15] H. E. Montgomery,[33] R. W. Moore,[47] M. Mostafa,[1] H. da Motta,[2] E. Nagy,[10] F. Nang,[25] M. Narain,[44] V. S. Narasimham,[15] H. A. Neal,[46] J. P. Negret,[5] S. Negroni,[10] D. Norman,[58] L. Oesch,[46] V. Oguri,[3] B. Olivier,[11] N. Oshima,[33] P. Padley,[59] L. J. Pan,[36] A. Para,[33] N. Parashar,[45] R. Partridge,[56] N. Parua,[9] M. Paterno,[51] A. Patwa,[52] B. Pawlik,[20] J. Perkins,[57] M. Peters,[32] O. Peters,[18] R. Piegaia,[1] H. Piekarz,[31] B. G. Pope,[47] E. Popkov,[38] H. B. Prosper,[31] S. Protopopescu,[53] J. Qian,[46] P. Z. Quintas,[33] R. Raja,[33] S. Rajagopalan,[53] E. Ramberg,[33] P. A. Rapidis,[33] N. W. Reay,[41] S. Reucroft,[45] J. Rha,[30] M. Rijssenbeek,[52] T. Rockwell,[47] M. Roco,[33] P. Rubinov,[33] R. Ruchti,[38] J. Rutherfoord,[25] A. Santoro,[2] L. Sawyer,[42] R. D. Schamberger,[52] H. Schellman,[36] A. Schwartzman,[1] J. Sculli,[50] N. Sen,[59] E. Shabalina,[22] H. C. Shankar,[15] R. K. Shivpuri,[14] D. Shpakov,[52] M. Shupe,[25] R. A. Sidwell,[41] V. Simak,[7] H. Singh,[30] J. B. Singh,[13] V. Sirotenko,[33] P. Slattery,[51] E. Smith,[55] R. P. Smith,[33] R. Snihur,[36] G. R. Snow,[48] J. Snow,[54] S. Snyder,[53] J. Solomon,[34] V. Sorín,[1] M. Sosebee,[57] N. Sotnikova,[22] K. Soustruznik,[6] M. Souza,[2] N. R. Stanton,[41] G. Steinbrück,[49] R. W. Stephens,[57] M. L. Stevenson,[26] F. Stichelbaut,[53] D. Stoker,[29] V. Stolin,[21] D. A. Stoyanova,[23] M. Strauss,[55] K. Streets,[50] M. Strovink,[26] L. Stutte,[33] A. Sznajder,[3] W. Taylor,[52] S. Tentindo-Repond,[31] J. Thompson,[43] D. Toback,[43] S. M. Tripathi,[27] T. G. Trippe,[26] A. S. Turcot,[53] P. M. Tuts,[49] P. van Gemmeren,[33] V. Vaniev,[23] R. Van Kooten,[37] N. Varelas,[34] A. A. Volkov,[23] A. P. Vorobiev,[23] H. D. Wahl,[31] H. Wang,[36] Z.-M. Wang,[52] J. Warchol,[38] G. Watts,[60] M. Wayne,[38] H. Weerts,[47] A. White,[57] J. T. White,[58] D. Whiteson,[26] J. A. Wightman,[39] D. A. Wijngaarden,[19] S. Willis,[35] S. J. Wimpenny,[30] J. V. D. Wirjawan,[58] J. Womersley,[33] D. R. Wood,[45] R. Yamada,[33] P. Yamin,[53] T. Yasuda,[33] K. Yip,[33] S. Youssef,[31] J. Yu,[33] Z. Yu,[36] M. Zanabria,[5] H. Zheng,[38] Z. Zhou,[39] Z. H. Zhu,[51] M. Zielinski,[51] D. Zieminska,[37] A. Zieminski,[37]

0031-9007/01/86(10)/1955(6)$15.00

V. Zutshi,[51] E. G. Zverev,[22] and A. Zylberstejn[12]

(D0 Collaboration)

[1]*Universidad de Buenos Aires, Buenos Aires, Argentina*
[2]*LAFEX, Centro Brasileiro de Pesquisas Físicas, Rio de Janeiro, Brazil*
[3]*Universidade do Estado do Rio de Janeiro, Rio de Janeiro, Brazil*
[4]*Institute of High Energy Physics, Beijing, People's Republic of China*
[5]*Universidad de los Andes, Bogotá, Colombia*
[6]*Charles University, Prague, Czech Republic*
[7]*Institute of Physics, Academy of Sciences, Prague, Czech Republic*
[8]*Universidad San Francisco de Quito, Quito, Ecuador*
[9]*Institut des Sciences Nucléaires, IN2P3-CNRS, Universite de Grenoble 1, Grenoble, France*
[10]*CPPM, IN2P3-CNRS, Université de la Méditerranée, Marseille, France*
[11]*LPNHE, Universités Paris VI and VII, IN2P3-CNRS, Paris, France*
[12]*DAPNIA/Service de Physique des Particules, CEA, Saclay, France*
[13]*Panjab University, Chandigarh, India*
[14]*Delhi University, Delhi, India*
[15]*Tata Institute of Fundamental Research, Mumbai, India*
[16]*Seoul National University, Seoul, Korea*
[17]*CINVESTAV, Mexico City, Mexico*
[18]*FOM-Institute NIKHEF and University of Amsterdam/NIKHEF, Amsterdam, The Netherlands*
[19]*University of Nijmegen/NIKHEF, Nijmegen, The Netherlands*
[20]*Institute of Nuclear Physics, Kraków, Poland*
[21]*Institute for Theoretical and Experimental Physics, Moscow, Russia*
[22]*Moscow State University, Moscow, Russia*
[23]*Institute for High Energy Physics, Protvino, Russia*
[24]*Lancaster University, Lancaster, United Kingdom*
[25]*University of Arizona, Tucson, Arizona 85721*
[26]*Lawrence Berkeley National Laboratory and University of California, Berkeley, California 94720*
[27]*University of California, Davis, California 95616*
[28]*California State University, Fresno, California 93740*
[29]*University of California, Irvine, California 92697*
[30]*University of California, Riverside, California 92521*
[31]*Florida State University, Tallahassee, Florida 32306*
[32]*University of Hawaii, Honolulu, Hawaii 96822*
[33]*Fermi National Accelerator Laboratory, Batavia, Illinois 60510*
[34]*University of Illinois at Chicago, Chicago, Illinois 60607*
[35]*Northern Illinois University, DeKalb, Illinois 60115*
[36]*Northwestern University, Evanston, Illinois 60208*
[37]*Indiana University, Bloomington, Indiana 47405*
[38]*University of Notre Dame, Notre Dame, Indiana 46556*
[39]*Iowa State University, Ames, Iowa 50011*
[40]*University of Kansas, Lawrence, Kansas 66045*
[41]*Kansas State University, Manhattan, Kansas 66506*
[42]*Louisiana Tech University, Ruston, Louisiana 71272*
[43]*University of Maryland, College Park, Maryland 20742*
[44]*Boston University, Boston, Massachusetts 02215*
[45]*Northeastern University, Boston, Massachusetts 02115*
[46]*University of Michigan, Ann Arbor, Michigan 48109*
[47]*Michigan State University, East Lansing, Michigan 48824*
[48]*University of Nebraska, Lincoln, Nebraska 68588*
[49]*Columbia University, New York, New York 10027*
[50]*New York University, New York, New York 10003*
[51]*University of Rochester, Rochester, New York 14627*
[52]*State University of New York, Stony Brook, New York 11794*
[53]*Brookhaven National Laboratory, Upton, New York 11973*
[54]*Langston University, Langston, Oklahoma 73050*
[55]*University of Oklahoma, Norman, Oklahoma 73019*
[56]*Brown University, Providence, Rhode Island 02912*
[57]*University of Texas, Arlington, Texas 76019*
[58]*Texas A&M University, College Station, Texas 77843*

[59]*Rice University, Houston, Texas 77005*
[60]*University of Washington, Seattle, Washington 98195*
(Received 6 September 2000)

We report on a study of the ratio of inclusive three-jet to inclusive two-jet production cross sections as a function of total transverse energy in $p\bar{p}$ collisions at a center-of-mass energy $\sqrt{s} = 1.8$ TeV, using data collected with the D0 detector during the 1992–1993 run of the Fermilab Tevatron Collider. The measurements are used to deduce preferred renormalization scales in perturbative $\mathcal{O}(\alpha_s^3)$ QCD calculations in modeling soft-jet emission.

DOI: 10.1103/PhysRevLett.86.1955 PACS numbers: 13.87.Ce, 12.38.Qk, 13.85.Hd

A primary manifestation of quantum chromodynamics (QCD) in $p\bar{p}$ collisions at a high center-of-mass energy ($\sqrt{s} = 1.8$ TeV) is the production of jets with large transverse momenta. Typically, the hard interaction of parton constituents of a proton and an antiproton produce two hard back-to-back jets. However, a fraction of the time, additional jets are also produced. In the absence of an all-orders QCD calculation, jet production rates as a function of jet energy are predicted by fixed-order calculations in perturbative QCD (pQCD). In this paper, we investigate the dependence of these calculations on the choice of parton distribution functions (pdf) and particularly renormalization and factorization scales.

We examine the ratio of inclusive three-jet production to inclusive two-jet production, which reflects the rate of gluon emission in QCD jet production processes. A three-jet cross section explicitly offers the opportunity to investigate a scale difference at a secondary vertex. Taking the ratio reduces systematic uncertainties.

Although this issue has inherent theoretical interest, it is also important because QCD multijet production is frequently a background to rare processes: phenomenologically confirmed prescriptions for renormalization scales are essential for predicting background rates and for designing efficient triggering schemes for rare processes at future colliders [1]. Last, when higher order QCD calculations become available, this ratio may be useful for providing another accurate measure of the strong coupling constant α_s.

The data used in this analysis, corresponding to an integrated luminosity of $\approx 10\ \mathrm{pb}^{-1}$, were recorded during the 1992–1993 Tevatron collider run. The D0 detector is described in detail elsewhere [2]. Jet detection primarily utilizes the uranium-liquid argon calorimeters, which have full coverage for pseudorapidity $|\eta| \leq 4$ where $\eta = -\ln[\tan(\theta/2)]$ and θ is the polar angle relative to the direction of the proton beam. Initial event selection occurred in two hardware trigger stages and a software stage. The first hardware trigger selected an inelastic $p\bar{p}$ collision as indicated by signals from trigger hodoscopes located near the beams on either side of the interaction region. The next stage required transverse energy above a preset threshold in calorimeter towers of 0.2×0.2 in $\Delta\eta \times \Delta\phi$, where ϕ is the azimuthal angle. Selected events were digitized and sent to an array of processors. Jet candidates were then reconstructed with a cone algorithm and the event recorded if any jet transverse energy (E_T) exceeded a specified threshold. Five such inclusive triggers had thresholds of 20, 30, 50, 85, and 115 GeV.

Jets were reconstructed offline using an iterative fixed-cone algorithm with a cone radius $\mathcal{R} = 0.7$ in $\eta - \phi$ space. The E_T of each jet was corrected for effects due to the underlying event, additional interactions, noise from uranium decay, the fraction of particle energy deposited outside of the reconstruction cone, detector uniformity, and detector hadronic response. A discussion of the jet algorithm, energy scale calibration, and resolution can be found in Refs. [3–5].

We measure the ratio of the inclusive three-jet to the inclusive two-jet cross section

$$R_{32} = \frac{\sigma_3}{\sigma_2} = \frac{\sigma(p\overline{p} \rightarrow n \text{ jets} + X;\ n \geq 3)}{\sigma(p\overline{p} \rightarrow m \text{ jets} + X;\ m \geq 2)}$$

as a function of the scalar sum of jet transverse energies ($H_T = \sum E_T^{\text{jet}}$). The measurement is performed for four distinct sets of selection criteria for all jets in the event: E_T thresholds of 20, 30, or 40 GeV for $|\eta_{\text{jet}}| < 3$, and $E_T > 20$ GeV for $|\eta_{\text{jet}}| < 2$. Three thresholds were chosen to study threshold dependence, and the minimum threshold was chosen to maximize statistics for which jet reconstruction efficiency was nearly 100%. Both in the data analysis and in the QCD calculation, a jet contributes to H_T and to the jet multiplicity if it passes all selection criteria and satisfies the E_T and η_{jet} requirements.

Figure 1 shows the ratio R_{32} as a function of H_T for E_T thresholds of 20, 30, and 40 GeV for $|\eta_{\text{jet}}| < 3$.

The five trigger samples listed in the figure contribute in separate regions of H_T, as indicated by the symbols. The distribution at the bottom of the figure shows the correlated systematic uncertainties for the 20 GeV threshold. This uncertainty is the maximum offset in the ratio obtained by a one standard deviation change in the correction to the jet energy scale. Error bars indicate statistical uncertainties (calculated using the appropriate binomial prescription for a statistically correlated ratio) as well as uncorrelated systematic uncertainties arising from all selection criteria. Table I displays the measurements in bins of H_T, showing the uncorrelated and correlated uncertainties for the four selection criteria.

JETRAD [6] is a next-to-leading-order Monte Carlo generator for describing inclusive multijet production. The

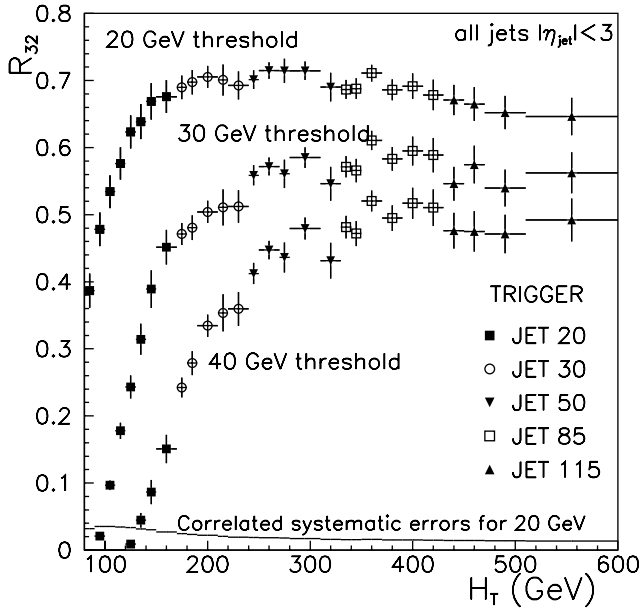

FIG. 1. The ratio R_{32} as a function of H_T for E_T thresholds of 20, 30, and 40 GeV ($|\eta_{\text{jet}}| < 3$). Error bars indicate statistical and uncorrelated systematic uncertainties, while the distribution at the bottom shows the correlated systematic uncertainty for the 20 GeV threshold.

generated 2-jet and 3-jet events are inclusive, and therefore the ratio of these cross sections should be equivalent to the measured R_{32}. CTEQ4M [7] pdf are used in the JETRAD simulations. The jet finding algorithm in JETRAD approximates the algorithm used in D0 data reconstruction. Jets generated by JETRAD are individually smeared according to known detector resolutions. Two partons are combined if they are within $\mathcal{R}_{\text{sep}} = 1.3\mathcal{R}$, as motivated by the separation of jets in the data [8] and, just as in the data, a jet is included if its E_T and η_{jet} meet the chosen selection criteria.

In pQCD, the renormalization procedure introduces a mass scale μ_R to control ultraviolet divergences in the calculations. A factorization scale μ_F, introduced to handle infrared divergences, is assumed to be equal to μ_R in all predictions described in this paper. QCD provides the evolution of α_s with μ_R, but not its absolute scale. Unless otherwise indicated, the renormalization scale $\mu_R = \lambda H_T$ will be used for the production of the two leading jets, where the constant λ, the coefficient of the hard scale, will have a nominal value of 0.3, but will be allowed to vary as described below. To study the possibility of having a different scale for the production of additional jets, the renormalization scale of the third jet is varied from $\mu_R^{(3)} = \lambda H_T$

TABLE I. Values of R_{32} with their uncorrelated and correlated uncertainties for the indicated jet E_T threshold and η_{jet} criteria. Uncorrelated uncertainties include statistical and uncorrelated systematic uncertainties added in quadrature.

H_T Range	$R_{32} \pm$ uncorrelated $\pm$ correlated uncertainty			
(GeV)	$E_T \geq 20$ GeV, $\lvert\eta\rvert < 2$	$E_T \geq 20$ GeV, $\lvert\eta\rvert < 3$	$E_T \geq 30$ GeV, $\lvert\eta\rvert < 3$	$E_T \geq 40$ GeV, $\lvert\eta\rvert < 3$
80–90	0.315 ± 0.019 ± 0.029	0.387 ± 0.025 ± 0.032		
90–100	0.408 ± 0.018 ± 0.031	0.478 ± 0.025 ± 0.035	0.021 ± 0.003 ± 0.011	
100–110	0.444 ± 0.018 ± 0.029	0.534 ± 0.024 ± 0.035	0.097 ± 0.007 ± 0.016	
110–120	0.496 ± 0.019 ± 0.027	0.576 ± 0.024 ± 0.034	0.178 ± 0.012 ± 0.018	
120–130	0.537 ± 0.021 ± 0.025	0.623 ± 0.025 ± 0.034	0.243 ± 0.017 ± 0.019	0.009 ± 0.004 ± 0.001
130–140	0.562 ± 0.025 ± 0.023	0.639 ± 0.026 ± 0.031	0.314 ± 0.023 ± 0.019	0.045 ± 0.011 ± 0.004
140–150	0.579 ± 0.027 ± 0.021	0.669 ± 0.027 ± 0.030	0.389 ± 0.028 ± 0.019	0.086 ± 0.018 ± 0.007
150–170	0.581 ± 0.025 ± 0.018	0.676 ± 0.024 ± 0.027	0.452 ± 0.026 ± 0.018	0.151 ± 0.021 ± 0.010
170–180	0.616 ± 0.016 ± 0.017	0.690 ± 0.018 ± 0.025	0.471 ± 0.016 ± 0.017	0.242 ± 0.015 ± 0.013
180–190	0.623 ± 0.017 ± 0.016	0.698 ± 0.018 ± 0.023	0.481 ± 0.018 ± 0.016	0.279 ± 0.018 ± 0.013
190–210	0.612 ± 0.016 ± 0.014	0.706 ± 0.016 ± 0.022	0.504 ± 0.017 ± 0.016	0.334 ± 0.016 ± 0.014
210–220	0.631 ± 0.025 ± 0.014	0.701 ± 0.023 ± 0.021	0.511 ± 0.027 ± 0.016	0.354 ± 0.028 ± 0.013
220–240	0.615 ± 0.023 ± 0.013	0.693 ± 0.021 ± 0.019	0.512 ± 0.024 ± 0.015	0.359 ± 0.025 ± 0.011
240–250	0.638 ± 0.014 ± 0.013	0.701 ± 0.014 ± 0.019	0.559 ± 0.015 ± 0.017	0.412 ± 0.016 ± 0.012
250–270	0.656 ± 0.012 ± 0.012	0.715 ± 0.012 ± 0.018	0.572 ± 0.013 ± 0.017	0.447 ± 0.014 ± 0.012
270–280	0.651 ± 0.020 ± 0.012	0.714 ± 0.018 ± 0.018	0.561 ± 0.021 ± 0.017	0.436 ± 0.022 ± 0.011
280–310	0.661 ± 0.015 ± 0.012	0.715 ± 0.014 ± 0.017	0.585 ± 0.015 ± 0.017	0.479 ± 0.016 ± 0.011
310–330	0.635 ± 0.023 ± 0.011	0.690 ± 0.021 ± 0.016	0.546 ± 0.025 ± 0.016	0.431 ± 0.027 ± 0.009
330–340	0.653 ± 0.015 ± 0.011	0.687 ± 0.014 ± 0.016	0.571 ± 0.016 ± 0.017	0.481 ± 0.017 ± 0.010
340–350	0.650 ± 0.016 ± 0.011	0.688 ± 0.015 ± 0.016	0.566 ± 0.017 ± 0.017	0.472 ± 0.019 ± 0.010
350–370	0.669 ± 0.014 ± 0.011	0.711 ± 0.013 ± 0.016	0.611 ± 0.014 ± 0.018	0.521 ± 0.016 ± 0.011
370–390	0.653 ± 0.017 ± 0.011	0.686 ± 0.016 ± 0.015	0.583 ± 0.018 ± 0.017	0.495 ± 0.019 ± 0.010
390–410	0.653 ± 0.020 ± 0.011	0.692 ± 0.019 ± 0.015	0.595 ± 0.022 ± 0.018	0.517 ± 0.023 ± 0.011
410–430	0.652 ± 0.024 ± 0.011	0.678 ± 0.023 ± 0.015	0.589 ± 0.026 ± 0.017	0.510 ± 0.027 ± 0.010
430–450	0.643 ± 0.023 ± 0.011	0.671 ± 0.023 ± 0.014	0.546 ± 0.025 ± 0.016	0.476 ± 0.027 ± 0.010
450–470	0.640 ± 0.027 ± 0.011	0.665 ± 0.025 ± 0.014	0.575 ± 0.028 ± 0.017	0.475 ± 0.030 ± 0.010
470–510	0.634 ± 0.026 ± 0.011	0.652 ± 0.025 ± 0.014	0.540 ± 0.027 ± 0.016	0.471 ± 0.029 ± 0.010
510–600	0.624 ± 0.029 ± 0.011	0.646 ± 0.028 ± 0.014	0.562 ± 0.031 ± 0.017	0.492 ± 0.032 ± 0.010

(same as for the leading jets) to a scale proportional to the E_T of the third jet $\mu_R^{(3)} \propto E_T^{(3)}$. Also, a scale proportional to the maximum jet transverse energy ($E_T^{\max}$) is studied, as this is a standard form used for comparisons of JETRAD to measured jet cross sections.

Figure 2 shows the measured R_{32} as a function of H_T for jet $E_T > 20$ GeV and $|\eta_{\text{jet}}| < 2$. The 20 GeV threshold has good sensitivity to scale in the JETRAD prediction and has reduced statistical uncertainty. The central rapidity region has the best understood jet energy uncertainties and correlations.

The plot contains four smoothed distributions corresponding to JETRAD predictions for the following renormalization prescriptions (shown for $\lambda = 0.3$):

$$\begin{aligned}
\text{(i)}\ \mu_R &= \lambda H_T \quad \text{for the two leading jets,}\\
\mu_R &= \lambda H_T \quad \text{also for the third jet (solid),}\\
\mu_R^{(3)} &= E_T^{(3)} \quad \text{for the third jet (dashed),}\\
\mu_R^{(3)} &= 2E_T^{(3)} \quad \text{for the third jet (dotted),}\\
\text{(ii)}\ \mu_R &= 0.6E_T^{\max} \quad \text{for all jets (dash-dot).}
\end{aligned}$$

All predictions demonstrate the same qualitative behavior as the R_{32} measurement, that is, a rapid rise below $H_T = 200$ GeV (associated with the kinematic threshold), a leveling off, then a slight drop at highest H_T (associated with the reduced phase space for additional radiation for high E_T jets). Although JETRAD predictions for the ratio are found to be insensitive to the choice of pdf, they do depend on the choice of $\mathcal{R}_{\text{sep}}$. Allowing $\mathcal{R}_{\text{sep}}$ to vary such that neighboring jets are all merged or all split causes a 3% decrease or increase in the ratio, respectively, with only a slight effect on the shape of the distribution in H_T.

For a quantitative comparison, we use a χ^2 covariance technique, defining

$$\chi^2 = \sum_{j=1}^{n} \sum_{i=1}^{n} (D_i - T_i) C_{ij}^{-1} (D_j - T_j),$$

where D_i and T_i represent the ith data and theory element, respectively, and $\mathbf{C^{-1}}$ is the inverse of the covariance matrix. This matrix incorporates uncorrelated uncertainties in the measurement and statistical uncertainties in the simulation, with correlated uncertainties included for the absolute jet energy in the data and for the uncertainty from resolution smearing in JETRAD (not shown explicitly in Fig. 2). Although some of the predictions do not visually overlap with the data, acceptable agreement is found for some scales because of the strong point-to-point correlations of the data uncertainties which are taken into account in the χ^2. Figure 3 shows the χ^2 per degree of freedom (χ^2/d.o.f.) as a function of the parameter λ, for the $E_T > 20$ GeV, $|\eta_{\text{jet}}| < 2$ selection criteria.

The degrees-of-freedom equal the number of data points (28). The horizontal line indicates the χ^2/d.o.f. obtained using the λ independent scale $\mu_R = 0.6E_T^{\max}$ for all jets. This scale yields good agreement with measurement (probability $p > 57\%$) for the $E_T > 20$ GeV criteria, but the χ^2 rises (and the corresponding probabilities decrease) for the higher E_T thresholds (not shown).

For λ-dependent scales, the best fit is specified by the λ that minimizes the χ^2. The scales proportional to $E_T^{(3)}$ for the third jet do not provide a good fit ($p < 5\%$) for any λ,

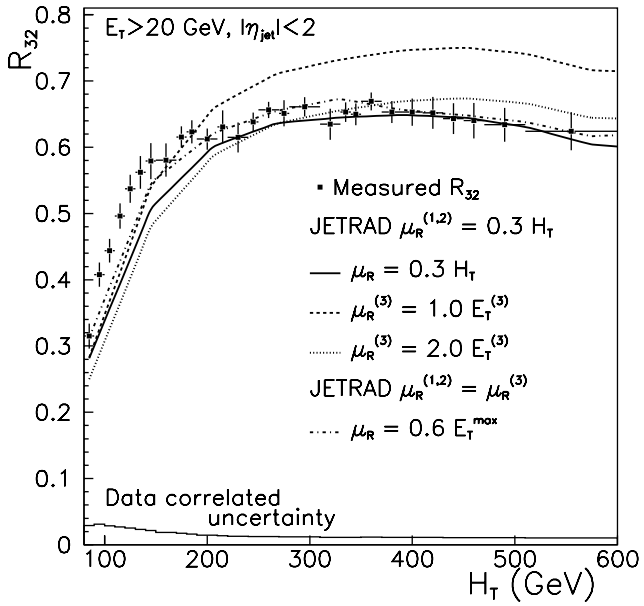

FIG. 2. The ratio R_{32} as a function of H_T, requiring jet $E_T > 20$ GeV and $|\eta_{\text{jet}}| < 2$. Error bars indicate statistical and uncorrelated systematic uncertainties, while the histogram at the bottom shows the correlated systematic uncertainty. The four smoothed distributions show the JETRAD prediction for the renormalization scales indicated in the legend.

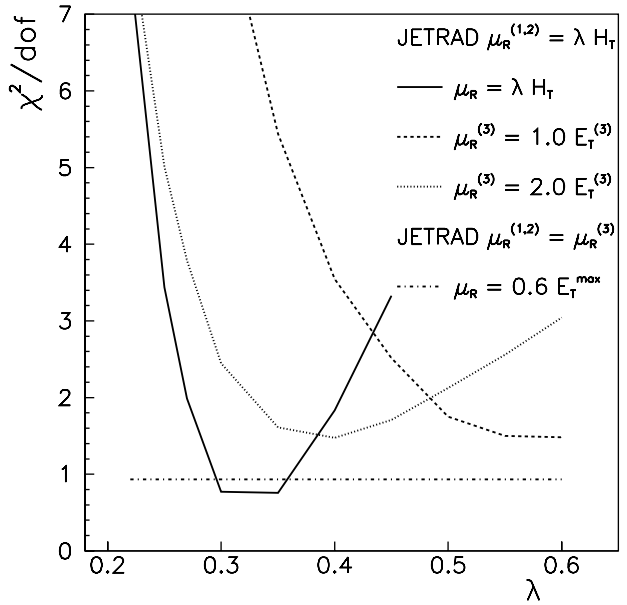

FIG. 3. χ^2/d.o.f. as a function of λ, comparing data to JETRAD predictions for several renormalization prescriptions for the $E_T > 20$ GeV, $|\eta_{\text{jet}}| < 2$ selection criteria.

as seen in Fig. 3. While there is fair agreement in the wider region of pseudorapidity $|\eta_{\text{jet}}| < 3$ for certain regions of λ (not shown), these do not correspond to the same values for different E_T thresholds, making the applicability of this scale prescription unsuitable for predicting production rates for additional jets.

The JETRAD prediction assuming a scale $\mu_R = \lambda H_T$ provides the best description of the data for λ between 0.30 and 0.35 ($p > 80\%$). Moreover, the χ^2 is also minimized in the $\lambda \approx 0.30$ region for the other selection criteria (not shown) making this scale choice the most robust of all the μ_R scales studied.

In conclusion, we have measured the ratio of the inclusive three-jet to the inclusive two-jet cross section as a function of total scalar transverse energy H_T and compared the results to JETRAD predictions. The greatest sensitivity to the choice of renormalization scale is for the lowest E_T threshold of 20 GeV. Although no prediction accurately describes the ratio through the kinematic threshold region, a single μ_R scale assumption in the calculation for all jets is found to adequately describe the rate of additional jet emission when correlated uncertainties are accounted for in a χ^2 comparison. Specifically, a scale of $\mu_R = \lambda H_T$ for all jets, where $\lambda = 0.3$, yields a prediction consistent with the measurement for all jet-selection criteria examined. A scale of $\mu_R = 0.6E_T^{\max}$ for all jets also provides a sufficient description at the lowest jet E_T threshold. The introduction of additional scales does not significantly improve agreement with the data.

We thank David Summers, Dieter Zeppenfeld, and Walter Giele for stimulating and helpful discussions. We also thank the staffs at Fermilab and at collaborating institutions for contributions to this work, and acknowledge support from the Department of Energy and National Science Foundation (U.S.A.), Commissariat à L'Energie Atomique and CNRS/Institut National de Physique Nucléaire et de Physique des Particules (France), Ministry for Science and Technology and Ministry for Atomic Energy (Russia), CAPES and CNPq (Brazil), Departments of Atomic Energy and Science and Education (India), Colciencias (Colombia), CONACyT (Mexico), Ministry of Education and KOSEF (Korea), CONICET and UBACyT (Argentina), A. P. Sloan Foundation, and the A. von Humboldt Foundation.

[1] D. Summers and D. Zeppenfeld, Phys. Lett. B **380**, 426 (1996).
[2] D0 Collaboration, S. Abachi *et al.,* Nucl. Instrum. Methods Phys. Res., Sect. A **338**, 185 (1994).
[3] L. Babukhadia, Ph.D. thesis, The University of Arizona, 1999 (unpublished).
[4] D0 Collaboration, B. Abbott *et al.,* Fermilab-Pub-00-216-E (to be published).
[5] D0 Collaboration, B. Abbott *et al.,* Nucl. Instrum. Methods Phys. Res., Sect. A **424**, 352 (1999).
[6] W. T. Giele, E. W. N. Glover, and David A. Kosower, Nucl. Phys. **B403**, 633 (1993).
[7] H. L. Lai *et al.,* Phys. Rev. D **55**, 1280 (1997), and references therein.
[8] B. Abbott *et al.,* Fermilab-Pub-97-242-E (unpublished).